



# Anatomical basis of lingual hydrostatic deformation

## Citation

Gilbert, R. J., V. J. Napadow, T. A. Gaige, and V. J. Wedeen. 2007. "Anatomical Basis of Lingual Hydrostatic Deformation." *Journal of Experimental Biology* 210 (23) (December 1): 4069–4082. doi:10.1242/jeb.007096.

## Published Version

10.1242/jeb.007096

## Permanent link

<http://nrs.harvard.edu/urn-3:HUL.InstRepos:36640546>

## Terms of Use

This article was downloaded from Harvard University's DASH repository, and is made available under the terms and conditions applicable to Other Posted Material, as set forth at <http://nrs.harvard.edu/urn-3:HUL.InstRepos:dash.current.terms-of-use#LAA>

## Share Your Story

The Harvard community has made this article openly available.  
Please share how this access benefits you. [Submit a story](#).

[Accessibility](#)

## Review

### Anatomical basis of lingual hydrostatic deformation

Richard J. Gilbert\*, Vitaly J. Napadow, Terry A. Gaige and Van J. Wedeen

*Department of Mechanical Engineering, Massachusetts Institute of Technology and the Athinoula A. Martinos Center for Biomedical Imaging, Massachusetts General Hospital, Cambridge, MA 02139, USA*

\*Author for correspondence (e-mail: rgilbert@mit.edu)

Accepted 27 July 2007

#### Summary

The mammalian tongue is believed to fall into a class of organs known as muscular hydrostats, organs for which muscle contraction both generates and provides the skeletal support for motion. We propose that the myoarchitecture of the tongue, consisting of intricate arrays of muscular fibers, forms the structural basis for hydrostatic deformation. Owing to the fact that maximal diffusion of the ubiquitous water molecule occurs orthogonal to the short axis of most fiber-type cells, diffusion-weighted magnetic resonance imaging (MRI) measurements can be used to derive information regarding 3-D fiber orientation *in situ*. Image data obtained in this manner suggest that the tongue consists of a complex juxtaposition of muscle fibers oriented in orthogonal arrays, which provide the basis for multidirectional contraction and isovolumic deformation. From a mechanical perspective, the lingual tissue may be considered as set of continuous coupled units of

compression and expansion from which 3-D strain maps may be derived. Such functional data demonstrate that during physiological movements, such as protrusion, bending and swallowing, hydrostatic deformation occurs via synergistic contractions of orthogonally aligned intrinsic and extrinsic fibers. Lingual deformation can thus be represented in terms of models demonstrating that synergistic contraction of fibers at orthogonal or near-orthogonal directions to each other is a necessary condition for volume-conserving deformation. Evidence is provided in support of the supposition that hydrostatic deformation is based on the contraction of orthogonally aligned intramural fibers functioning as a mechanical continuum.

Key words: magnetic resonance imaging, myoarchitecture, tissue mechanics.

#### Hydrostatic model of lingual deformation

The designation of a tissue as a muscular hydrostat indicates that the tissue has the ability to both create and supply the structural support for motion (Kier and Smith, 1985; Smith and Kier, 1989; Nishikawa, 1999). Characteristically, such a tissue capitalizes on its high water content, and hence incompressibility, to modify its form without a change of volume. It is the underlying hypothesis of this review that the mammalian tongue should appropriately be classified as a muscular hydrostat, and that its hydrostatic properties are attributable to the presence of muscle fibers and fiber arrays orthogonally aligned with each other.

A constant morphological feature of all muscular hydrostats in nature is the presence of muscle fiber populations aligned both perpendicular (transverse, vertical, circumferential or radial directions) and parallel (longitudinal direction) to the organ's long axis. For example, muscular hydrostats that principally perform bending motions, such as the snake, which flicks its chemoreceptor-laden organ to sense its prey, tend to have longitudinal fibers further away from the longitudinal axis and produce a greater moment about the bending axis. If the principal function of the longitudinal fibers is to produce

retraction, as is the case for certain reptiles, such as the monitor lizard *Varanus exanthematicus* and garter snake *Thamnophis*, and mammals, such as the pangolin (scaly anteater) *Manis*, these muscles are generally located along the central axis of the organ. For those muscular hydrostats with muscular elements oriented helically about the organ's long axis, such as the elephant trunk, the fibers characteristically produce both positive and negative torsion and are positioned to maximize the torsional moment during grasping. The mammalian tongue exhibits an enormous degree of mechanical versatility. The scaly anteater (*Manis*) has the distinction of being the tongue length champion, at least relative to its body size. Its tongue characteristically extends back, posterior to the sternum, to an attachment on a specialized xiphoid cartilage. The tongue's caudal cross-section is composed of longitudinal fibers surrounded by circular fibers (perpendicular to the long axis). The xiphoid plate is analogous to the hyoid bone in other mammals as it is an attachment for the genioglossus and geniohyoid (protractor muscles), and sternohyoid (retractor muscle), and is used by the *Manis* for scraping termites off the sticky body of the tongue so that they may be placed in the esophagus. The extrinsic sternohyoid attaches to both the xiphoid process and caudally all the way to

the right iliac fossa of the pelvis. The overall tongue length for the *Manis* is typically around 70 cm, which is rather long for an animal whose body length is only 120–140 cm. The performance of the human tongue during swallowing is also an important example of hydrostatic deformation (Miller, 1982). During the swallow, a synchronized series of deformations results in the transport of ingested food from the mouth to the esophagus. Immediately following ingestion, the food is physically modified through a set of actions, termed mastication, which produces a shaped bolus of semi-solid or fluid consistency (Thexton, 1992; Palmer et al., 1992; Hiiemae and Palmer, 1999). This process incorporates tethered motions of the tongue, hyoid bone and jaw in species-specific patterns (Smith, 1986; Thexton and McGarrick, 1988; Thexton and McGarrick, 1994; Herrell et al., 1996; Thexton and Hiiemae, 1997). Once the bolus has been configured, oral stage swallowing ensues, which includes the creation and optimization of the accommodating cavity by patterned deformation, followed by retrograde propulsion (Gilbert et al., 1998a) (Fig. 1). On delivery of the bolus to the pharynx, the pharynx displaces in a superior direction, producing a cylinder-like flow chamber (Flaherty et al., 1995). Propagating pharyngeal contractions then combine with anterior pharyngeal displacement to produce an orderly flow of the bolus from the pharynx, past the occluded airway and into the esophagus (Maddock and Gilbert, 1993; Paydarfar et al., 1995; Kahrilas et al., 1992).

The mammalian tongue is unique inasmuch as its myoarchitecture is organized into both intrinsic and extrinsic fiber populations, which function synergistically. In general, the contractions produced by the intrinsic elements are augmented and modified by extrinsic muscular elements that tether the tongue to the surrounding skeletal structure. Historically, it was thought that extrinsic muscles alter tongue position, while intrinsic muscles alter tongue shape – a misconception that has, to some extent, persisted to the present day. A more likely scenario may be that the extrinsic and intrinsic muscles work in concert to produce changes in both tongue position and shape, thus maintaining the hydrostatic condition. For example, the extrinsic genioglossus merges with fibers of the intrinsic verticalis muscle, contributing to anterior protrusion and bolus accommodation in swallowing. During the bolus propulsion stage of swallowing, the extrinsic styloglossus muscle pulls the

posterior tongue retrograde – aiding hydrostatic expansion by the intrinsic transversus muscle and propelling the swallowed bolus into the pharynx. It has been theorized that muscular hydrostats optimize speed and flexibility during deformation by such synergistic muscular activity, while sacrificing force production. By comparison, force production may be maximized in non-hydrostatic systems by large moment arms juxtaposed about a joint supported by a bony skeleton. The African pig-nosed frog *Hemissus marmoratum* has the remarkable ability to elongate its tongue by as much as 100% as well as to bend through an angle exceeding 180°. In the life of *H. marmoratum*, this ability is important for achieving the requisite degree of lingual motor control to capture its prey. It is notable that this species lacks pure intrinsic muscles and thus elongation can only occur by the action of extrinsic muscles, whose fiber angles within the tongue are oriented perpendicular to the long axis of the tongue. In fact, elongation is accomplished by the coordinated activity of two compartments of the genioglossus muscle, one in which the muscle fibers are arranged parallel to the long axis, termed the genioglossus longitudinalis, and one in which the fibers are arranged dorsoventrally within the tongue, termed the genioglossus dorsoventralis. Nishikawa and colleagues (Nishikawa et al., 1999) proposed that the simultaneous actions of these orthogonally oriented (but extrinsically attached) muscle systems within the body of the tongue of *H. marmoratum* allow its dramatic capacity for elongation and bending.

We contend that the ability of the mammalian tongue to carry out its large array of physiological motions is based on its muscular anatomy, which is composed of complex fiber arrays aligned at various angles orthogonal to the direction of deformation. We propose that these fiber alignments comprise the structural underpinnings for hydrostatic deformation and are thus fundamental to the generation of lingual force.

### Lingual myoarchitecture and hydrostatic deformation

The tongue is a large muscular organ that fills the majority of the oral cavity in most mammals, except for some of the Odontoceti (toothed whales), Rodentia and Ornithorhynchus (duck-billed platypus). The tongue's phylogenetic origins date back to prehistoric fish, where it first appears as a rudimentary organ. By its morphology, the tongue may be considered as an appendage of the hyoid part of the branchial skeleton and thus

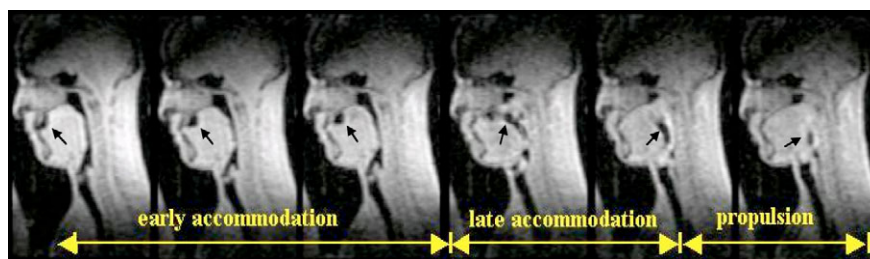
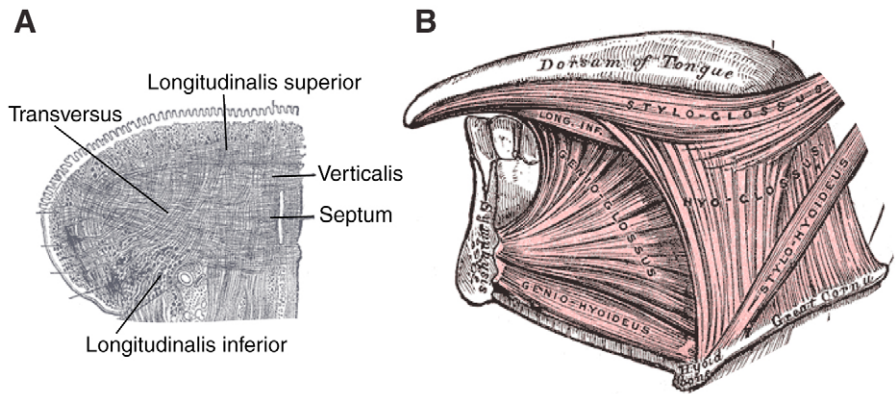


Fig. 1. Patterns of lingual deformation during swallowing. The swallow is portrayed as a sequence of mid-sagittal images of lingual deformation acquired at 10 Hz using magnetic resonance imaging (MRI, TurboFlash). Shown is a series of images depicting the early accommodation, late accommodation and propulsion phases of the swallow. During early accommodation, an accommodating concavity is created in which the bolus (depicted as a black signal void in the current image sequence) is situated in the anterior oral cavity. With conversion to late accommodation, the concavity is deepened and transferred posteriorly. During the propulsive phase of the swallow, the bolus is propelled retrograde from the oral cavity to the pharynx. Arrow indicates location of the fluid bolus.

Fig. 2. Tongue anatomy: classical definitions. (A) Shown here are the intrinsic muscles – that is, the longitudinalis (superior and inferior), transversus and verticalis muscles – in a coronal cross-section of the mammalian tongue. By definition, the intrinsic muscles have no bony attachments, being wholly contained within the tongue. (B) As conventionally defined, the extrinsic muscles insert into the tongue from a superior direction (palatoglossus), postero-superior direction (styloglossus), postero-inferior direction (hyoglossus) and antero-inferior direction (genioglossus). The genioglossus is a large muscle comprising the bulk of the posterior tongue, which originates at the mental spine of the mandible and enters the tongue from below. As noted in the text, while the extrinsic muscles are distinct in their anatomy and physiology at the points of bony attachment, they merge with the intrinsic fibers at the point of insertion into the tongue proper.



can be viewed as a variation on the anatomy of the floor of the mouth. In fact, the simplest form of the vertebrate tongue, seen in some birds and snakes, consists of an extension of the entoglossal process, considered to be a part of the hyoid process. The cartilaginous tongue so configured may be moved simply by moving the hyoid bone. Muscles such as the sternoglossus connect the sternum to the tongue, with some fibers having connections to the hyoid bone. The human tongue does not have a sternoglossus muscle, but retains a connection to the hyoid bone through the hyoglossus muscle, which is connected to the sternum through the sternohyoid muscle. Thus, the human tongue is still influenced by hyoid motion, yet its complex musculature and fine neurological control grants this organ substantial mechanical independence. During the course of human development, the size of the human tongue reflects its physiological function. At birth and during early maturation, the tongue is disproportionately large relative to its surrounding structures. In a newborn infant, the tongue fills the oral cavity, presumably related to the increased need for the tongue during suckling. With development of the infant, the size of the oral cavity increases faster than the size of the tongue, resulting in the appearance of a 'masticatory space' superior to the tongue. With this development, the tongue no longer maintains resting contact with the hard palate, although contact with the soft palate is maintained, allowing separation of the mouth from the pharynx.

The musculature of the tongue is classically divided into two types of muscle, intrinsic and extrinsic (Fig. 2). Intrinsic muscles are myofiber populations wholly contained within the body of the tongue, unconnected to any external bony attachments. In contrast, extrinsic muscles have one bony attachment outside the tongue proper. The intrinsic muscles include the superior and inferior longitudinalis, the transversus and the verticalis muscles. The transversus, verticalis and longitudinalis muscles also extend to the posterior tongue, where they are merged with the extrinsic muscles. These muscles enter the tongue proper from a superior direction (palatoglossus), postero-superior direction (styloglossus), postero-inferior direction (hyoglossus) and antero-inferior direction (genioglossus). The genioglossus comprises the bulk of the posterior tongue and enters the tongue in a fan-like projection, originating at the mental spine of the mandible. The

tongue rests on a muscular floor composed of the geniohyoid muscle, which runs in the mid-sagittal plane from the mental spine of the mandible to the body of the hyoid bone, and the mylohyoid, which runs from the mylohyoid line of the mandible to the raphe and body of the hyoid bone. It should, however, be recognized that the distinction between intrinsic and extrinsic musculature tends to break down at the point of extrinsic muscle insertion into the tongue body. As a result, we contend that it is more appropriate to consider the tongue not as a set of discretely parcellated muscles but rather as a continuous array of fibers with varying orientations and mechanical properties.

It is generally believed that the direction of skeletal muscle contraction is dictated by the principal orientation of its fibers. While the determination of a muscle's principal fiber direction is straightforward in tissues where the fibers are aligned along a single spatial axis, for example, the muscles of the extremities, the process is considerably more complicated in tissues where fibers are aligned along multiple axes, for example, the tongue, heart and GI tract. The fact that the tongue comprises an extensive array of interdigitating fibers contributes to the organ's almost limitless number of possible deformations. Deriving accurate information regarding lingual muscle fiber orientation has classically relied on meticulous dissection and multislice reconstruction, an approach that is both laborious and ill-posed in the case of the tongue. The difficulty stems from the inability of histology, an inherently 2-D technique, to resolve through plane fiber angle and thus allow 3-D reconstruction (McLean and Prothero, 1987; McLean and Prothero, 1992). With these caveats in mind, previous investigations have been instrumental in providing information regarding lingual configuration changes during motion, and from these models the details of fiber relationships, distribution of fiber types and innervation have been inferred (DePaul and Abbs, 1996; Mu and Sanders, 1999; Takemoto, 2001). A particularly compelling aspect to the study of lingual anatomy is the fact that the extrinsic muscles appear to merge seamlessly with the intrinsic musculature, thus confounding the definition of distinct muscles within the body of the tongue. For example, as the genioglossus muscle fans superiorly into the tongue's intrinsic core, its fibers merge with verticalis muscle fibers, sometimes extending all the way to the superior longitudinalis. Continuum modeling, which recognizes the musculature as a continuous array of elements,



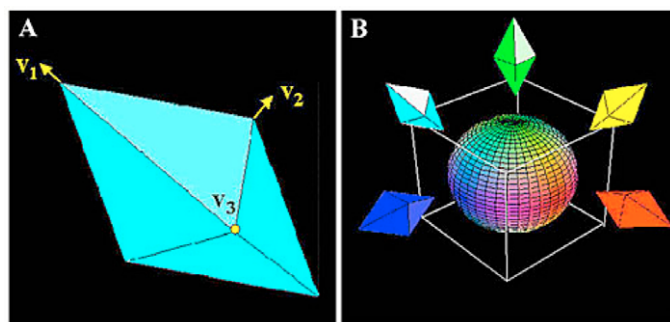


Fig. 3. Generation of the diffusion tensor. The physical basis for diffusion-weighted imaging is that a magnetic gradient is first dephased and then rephased, and the resulting loss of signal coherence (yielding signal attenuation) represents diffusive motion in the direction of the applied gradient. The set of spatially arrayed diffusion coefficients may be viewed as a second-order tensor, so constituting a method for visualizing 3-D diffusivity in space. The 3-D diffusion tensor may be computed for each voxel and visualized as individual octahedra (A) whose axes are scaled by the size of the eigenvalues and oriented along the corresponding eigenvectors. The principal eigenvector,  $\mathbf{V}_1$ , corresponds to the direction of greatest diffusion, and is equivalent to the principal fiber direction. Octahedra may then be color coded based on the principal eigenvector  $\{x, y, z\}$  mapped to the red–green–blue color space:  $\{|\mathbf{V}_{1x}|\}$  (B).

may thus be a more valid way to conceive the tongue's myoarchitecture. Both intrinsic and extrinsic lingual fibers may be arrayed within the tissue to generate a large variety of shapes by virtue of the tissue's hydrostatic properties. The structural components of each element may further be considered as a hierarchical organization of individual myofibers and collagen-delimited fiber bundles, allowing the tissue to be defined simultaneously at macroscopic (discrete regions within a tissue) and microscopic (individual myofibers and fiber bundles) resolutions. Diversity of physiological function may be derived from the anatomical relationships between fibers and fiber bundles, as well as regional differences of innervation, excitation–contraction coupling and muscle fiber type.

An alternative method for imaging lingual myoarchitecture employs non-invasive diffusion-based magnetic resonance imaging (MRI) (Stejskal, 1965). Owing to the fact that maximal diffusion of the ubiquitous water molecule is aligned with fiber direction, diffusion measurements can be used to derive information regarding 3-D fiber orientation *in situ* (Basser et al., 1994; Gmitro and Alexander, 1993; Hajnal et al., 1991; Moseley et al., 1991; Wu et al., 1993). Diffusion is a physical property representing the random translational motion of water molecules and is modified principally by the location of diffusional barriers. In muscular tissue, diffusion is greatest along the direction of individual or populations of fibers due to their elongated and cylindrically symmetrical geometry. Signal attenuation receives contributions from both intracellular and extracellular fluid; however, the explicit shape of muscle cells insures that both components induce maximal attenuation along the long axis of the myofiber. As a result of these considerations, diffusion measurements can be used to derive information regarding 3-D fiber orientation *in situ*. This general approach allows us to resolve the relatively complex fiber orientation of

tissues at multiple spatial scales. The use of diffusion tensor fields allows for the derivation of a single principal fiber direction for each imaging unit (generally in the scale of  $\text{mm}^3$ ), or voxel, thus allowing us to generate a virtual anatomical display of the whole bovine tongue (Gilbert et al., 1998b; Wedeen et al., 2001).

In order to recover diffusion data from MRI, transverse magnetization is first dephased and then rephased under the influence of a spatially dependent magnetic field gradient. This 'echo' completely rephases the original magnetization, except for any diffusive motion that occurs along the direction of the applied gradient. Molecular diffusion is thus reflected by a loss of signal coherence and incomplete refocusing, yielding net attenuation of the MRI signal. From the extent of signal attenuation, a diffusion coefficient may then be calculated. The derivation of a set of diffusion coefficients (controlled by spatially variant applied magnetic gradients) results in a unique array of 3-D data for each voxel. Quantitatively, this symmetrical second-order tensor can be conceived as a function of signal attenuation by Eqn 1:

$$\ln \left( \frac{S_b}{S_0} \right) = - \sum_{i=1}^3 \sum_{j=1}^3 b_{ij} D_{ij}, \quad (1)$$

where  $S_b$  is the signal-attenuated image,  $S_0$  is the unattenuated image,  $b_{ij}$  is the  $ij$  component of the b-matrix, and  $D_{ij}$  is the  $ij$  component of the diffusion tensor (Basser, 1994). The b-matrix is related to the direction-dependent diffusion sensitization and is expressed as  $b = \int \mathbf{k}^T \mathbf{k} dt$ , where the reciprocal space vector,  $\mathbf{k}$ , can be expressed as a function of the proton gyromagnetic ratio and the 3-D diffusion sensitization gradient vector. In order to efficiently span 3-D space with the diffusion sensitization gradients, seven images are acquired; six with gradient vectors towards the unopposed edge centers of a theoretical cube, and one unattenuated image. This yields a system of linear equations, which can be solved for the diffusion tensor,  $\mathbf{D}$ , in the  $x$ – $y$ – $z$  coordinate system. This tensor may then be transformed by solving  $\mathbf{D}\mathbf{v} = \lambda\mathbf{v}$  in order to derive the diffusion tensor in the eigen coordinate system. The complete 3-D diffusion tensor may be computed for each image voxel and visualized as individual octahedra, whose axes are scaled by the size of the eigenvalues and oriented along the corresponding eigenvectors. Within the eigen coordinate system, the principal eigenvector,  $\mathbf{v}_1$ , corresponds to the direction of greatest diffusion, or principal fiber direction, and was the major axis of the octahedron. The eigenvalues and eigenvectors for each diffusion tensor represent the magnitude and direction of maximal proton diffusivity, respectively (Fig. 3). Diffusion tensor anisotropy may also be depicted in terms of the oblateness of the diffusion tensor, and hence the homogeneity of fiber orientation within a voxel. By this method, homogeneous tissue where most of the myofibers are oriented along the same axis will have a high anisotropy index and heterogeneous tissue with different myofiber orientations (e.g. multiple intertwined or overlaid fiber populations) will have a low anisotropy index.

A rendering of lingual fiber myoarchitecture (Wedeen et al., 2001) is depicted in Fig. 4 for a mid-sagittal slice of the bovine tongue. In this image, the fiber populations are represented by

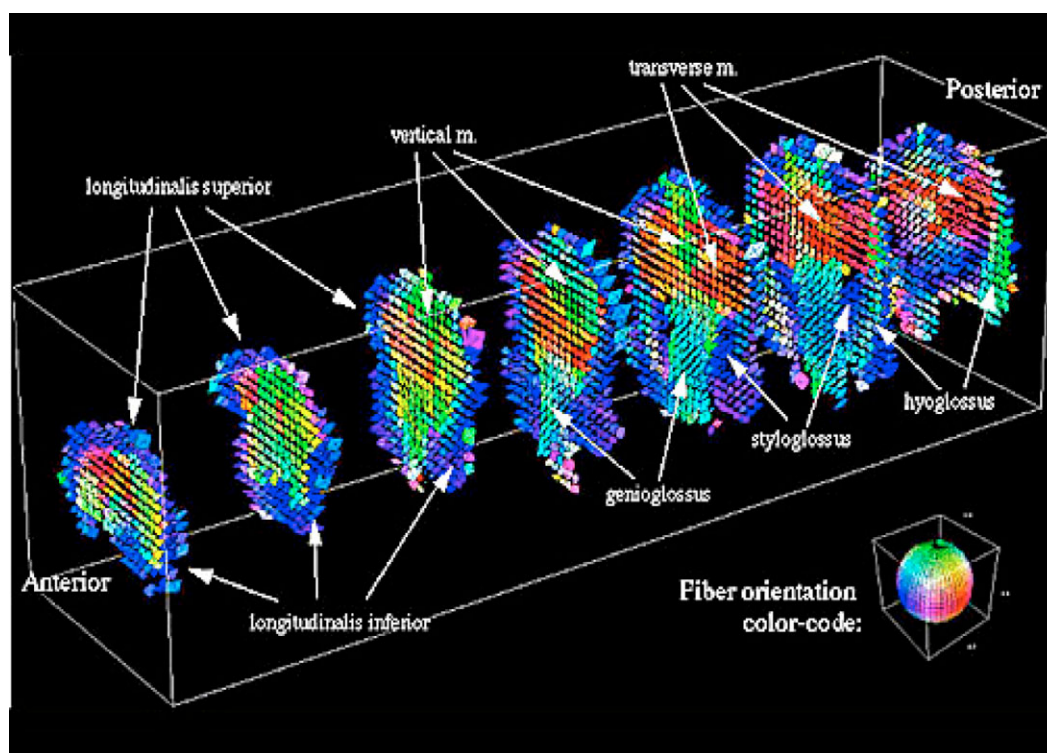


Fig. 4. 3-D multislice diffusion tensor MRI representation of the bovine tongue. Coronal slices comprising the bovine tongue obtained by diffusion tensor imaging are shown, with muscle components identified. At each voxel, an octahedron is placed whose shape approximates the local diffusion tensor. The fiber orientation corresponds to the octahedron's long axis and its color to the 3-D orientation. The color code is shown in the color sphere (inset). The sheath consisting of superior and inferior longitudinal muscles is blue, corresponding to its longitudinal fiber orientation, and the tongue core is red and green, corresponding, respectively, to horizontal and vertical fiber orientations, whereas the extrinsic genioglossus and hyoglossus muscles are oblique, and thus coded blue–green. (Reproduced with permission from Wedeen et al., 2001.)

color-coded octahedra. These results demonstrate that fibers which are aligned parallel to the mid-sagittal imaging plane originate in the postero-inferior region of the tongue, and radiate in the anterior and superior direction, ultimately merging with vertically oriented fibers towards the periphery of the tongue. Through-plane fibers, on the other hand, are located predominantly in the anterior and superior regions of the tongue. Fibers localized to the postero-inferior tongue display a highly uniform and parallel organization, whereas fibers localized to the antero-superior tongue show progressively less uniformity of fiber orientation. Owing to the distinction in the anterior tongue between the orthogonal core fibers and the longitudinal sheath fibers, this tissue region may be further analyzed by graphically depicting its 2-D architecture (Fig. 5). In this data rendering,  $\mathbf{v}_1, \mathbf{v}_2$  constitutes the face of a flattened cylinder, representing maximal angular dispersion of fiber angles. These data depict a striking contrast between the core fibers, consisting of the vertical and transverse fibers, and sheath fibers formed by the longitudinalis muscles. The fiber planes of the tongue sheath are concentric with the surface of the tongue and locally parallel to the adjacent surface of the tissue. This approach resolves the constituent muscles of the tongue based on the principal directions of its fibers and the angular dispersion of these fibers within the imaged element. By this formulation, the principal fiber orientation at each location in the image corresponds to the leading eigenvector of the diffusion tensor,

whereas the second eigenvector identifies the orientation of maximum fiber angle dispersion in each voxel. These results are consistent with the hydrostat model in that they explicitly portray crossing vertical and horizontal fibers in the lingual core, which may cause, by simultaneous contraction (with conservation of volume), the tongue to protrude in the anterior–posterior axis, orthogonal to the plane of these fibers. The tongue core and sheath comprise a functionally opposed pair, in which protrusion produced by bidirectional contraction of the core muscles is opposed by the retraction produced by unidirectional contraction of the longitudinal sheath muscles.

The fact that diffusion tensor imaging yields only one principal fiber direction per voxel, however, limits its ability to discern fiber direction where fibers cross at the scale of the individual voxel, as is typical for the tongue. Diffusion spectrum imaging (DSI) (Wedeen et al., 2000; Lin et al., 2003; Tuch et al., 2003) is a method for determining the alignment of geometrically heterogeneous muscle fiber populations, for which the complete 3-D spin displacement function may be determined within a single voxel as small as  $500 \mu\text{m}^3$ . DSI involves the acquisition of numerous diffusion-weighted magnetic resonance images per spatial unit, each with a different diffusion-weighting gradient value and angularity. This extension of the prior diffusion-weighted techniques thus allows the quantification of fiber direction in the case of the complex myoarchitectural patterns (Gilbert et al., 2006). DSI yields an

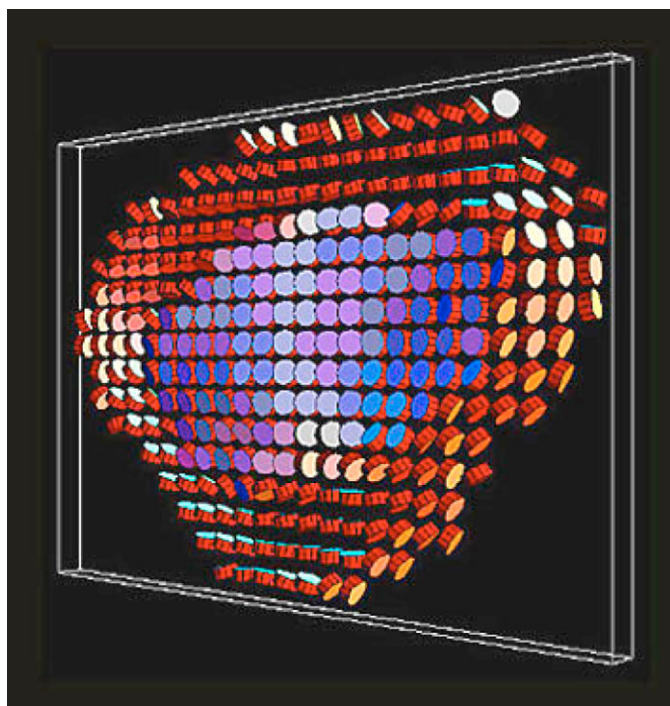


Fig. 5. Representation of planar diffusion for the bovine tongue (coronal imaging slice). The orientation of the diffusion tensor's greatest two eigenvectors, the plane of maximum intra-voxel fiber angle dispersion, is represented by the end-planes of graphic cylinders derived from a coronal slice of the lingual core. Contrast was seen between the tongue core, where the planes of fiber angle dispersion were transverse to the antero-posterior axis of the tongue, and the tongue sheath, where these planes were approximately parallel to the nearby tongue surface. (Reproduced with permission from Wedeen et al., 2001.)

ensemble probability density function (PDF) for the set of molecular displacements occurring as a function of molecular motion; in effect, the average probability of a spin undergoing a given displacement over a given diffusion time. By measuring the microscopically resolved 3-D diffusion functions, DSI depicts complex fiber relationships as the multimodal behavior of the PDF within a macroscopically resolved voxel of tissue. In DSI, diffusion-weighted images are acquired for a sphere of  $\mathbf{q}$  vectors with indexed values in a Cartesian grid in  $\mathbf{q}$  space, in order to produce a 3-D probability distribution. The relationship between the diffusion attenuation and a diffusion-weighting gradient  $\mathbf{g}$  of duration  $\delta$  is depicted by Eqn 2:

$$M(\mathbf{q}, \Delta) = M(0, \Delta) \int \bar{P}_s(\mathbf{R}|\Delta) \exp(i\mathbf{q} \cdot \mathbf{R}) d\mathbf{R}, \quad (2)$$

where  $\mathbf{q}$  is equal to  $\gamma \mathbf{g} \delta$ ,  $\gamma$  is the proton gyromagnetic ratio for a water molecule,  $M$  is the signal intensity,  $\Delta$  is the diffusion time,  $\mathbf{R}$  is the diffusion distance and  $\bar{P}_s$  is the average PDF. In DSI, diffusion-weighted images are acquired for a sphere of  $\mathbf{q}$  vectors with indexed values in a Cartesian grid in  $\mathbf{q}$  space, in order to produce a 3-D probability distribution. The spacing between  $\mathbf{q}$  vectors defines the field of view and the maximum  $\mathbf{q}$  vector defines the resolution of the PDF. In order to make visualization more clear, the 3-D diffusion function may be reduced by integrating  $\bar{P}_s$  weighted radially by the magnitude

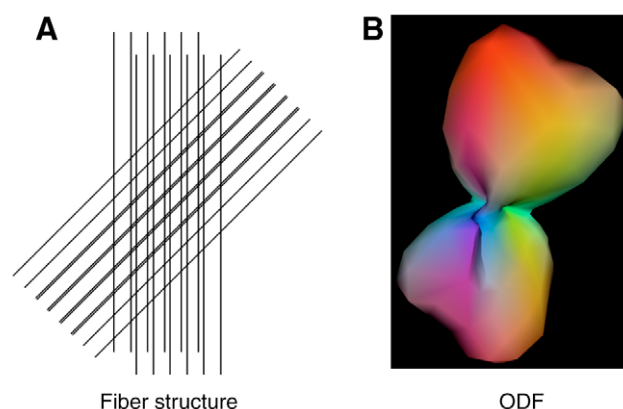


Fig. 6. Physical basis for diffusion spectrum imaging (DSI). DSI is a high resolution diffusion-weighted imaging technique which determines the complete spin displacement function by acquiring a large number of images with varying diffusion weighting and angularity. This results in the generation of a probability density function (PDF) for the entire set of possible molecular displacements, and thus depicts the set of principal fiber orientations based on the properties of the diffusion maxima. (A) Two sets of model fibers drawn with arbitrary angular separation. (B) In order to simplify the visualization of 3-D diffusion, the PDF is converted to an orientational diffusion function (ODF), which provides a probability distribution for diffusion for a set of angular directions, weighted by the magnitude of the diffusion.

of  $\mathbf{R}$ . This new data set is termed the orientational distribution function (ODF) and provides a probability distribution for diffusion for a set of angular directions, weighted by the magnitude of the diffusion (Fig. 6).

Fig. 7 demonstrates variations in the patterns exhibited by crossing fibers in the anterior core of the tongue in three adjacent axial imaging slices (A–C). Fig. 9D of Gilbert et al. (Gilbert et al., 2006) depicts a single voxel at high magnification showing the convergence of three fiber populations, oriented principally in the vertical, transverse and longitudinal directions. Fig. 9E of the same study depicts a single population of fibers, aligned at an angle between the longitudinal and the vertical. Fig. 9F of the study demonstrates two crossing fiber populations, oriented orthogonal to each other in the vertical and transverse directions. The use of DSI distinguishes between regions consisting of crossing and non-crossing fiber populations, and explicitly allows angular quantification of crossing fiber populations. Based on the above formulations, it may be readily considered that the extent to which such crossing fibers are present in a given region impacts upon its ability to undergo hydrostatic deformation. These data specifically demonstrate that the tongue tissue may be delineated into regions defined by the degree to which fibers are homogeneously aligned, i.e. without significant crossing fiber populations at the voxel resolution, or heterogeneously aligned, i.e. exhibiting two to three crossing fiber populations. It is further shown that regions exhibiting extensive crossing merge in an almost seamless manner with regions exhibiting homogeneity of fiber alignment, thus reaffirming the concept that the lingual musculature, and perhaps numerous other muscle systems, are best conceived as mechanical continua



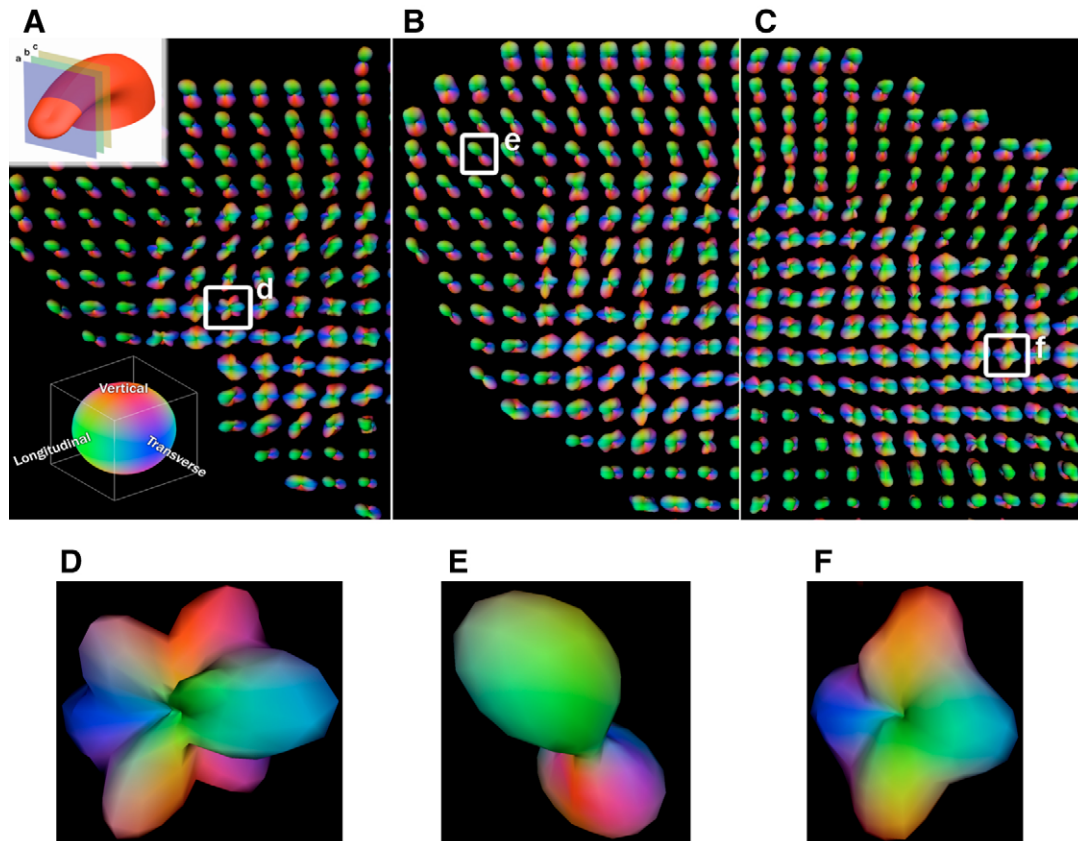


Fig. 7. Diffusion spectrum imaging slices obtained from the bovine tongue (axial orientation). Shown are adjacent axial slices of the bovine tongue (A–C, anterior to posterior) obtained by DSI and depicted as a set of 3-D ODFs. Principal fiber directions are color coded (see inset in A), with green indicating the tissue's longitudinal axis, red the vertical axis and blue the transverse axis. (D–F) Selected regions of a single voxel at increased magnification to illustrate ODF detail. (D) Single voxel image showing three distinct crossing fiber populations. (E) Single voxel image showing a single population of fibers, oriented diagonally inward towards the tip of the tongue, exhibiting longitudinal (green) and vertical (red) alignment. (F) Single voxel image showing two crossing fiber populations, orthogonal to each other. (Reproduced with permission from Gilbert et al., 2006.)

rather than the simple juxtaposition of discrete muscle populations. Given the voxel-scale complexity of the tongue, and the continuous nature of the contractions underlying its deformations, quantifications of the angular relationships involving orthogonally aligned fibers should have value in the derivation of structure–function relationships.

From the above, it may be surmised that lingual myoarchitecture arises from the juxtaposition of muscle fiber arrays obliquely oriented to each other. According to the hydrostat hypothesis, the existence of crossing fibers allows for the possibility of synchronized multidirectional contraction and isovolemic deformation. Similarly oriented fibers may act *en masse* as a contractile unit or promote specific patterns of regional contraction. For example, during human swallowing, the serial alternation of transversus and verticalis bundles allows the bolus-accommodating depression in the tongue to translate posteriorly, therefore bringing food deeper into the oropharynx prior to retrograde propulsion. Both fiber populations are necessary, as verticalis muscle contraction allows for a depression to be formed, while transversus muscle contraction creates expansion towards the hard palate. The presence of structural complexity, where fibers are aligned simultaneously

along multiple spatial axes, thus serves as an anatomical prerequisite for hydrostatic deformation.

#### Mechanical evidence supporting hydrostatic lingual deformation

Designating a tissue as a muscular hydrostat implies that the tissue, by its highly aqueous nature, has the ability to deform isovolemically. In order to achieve this function, the tissue must possess muscle fibers that are arrayed across a large spectrum of angles and exhibit the capacity for multidirectional contraction. Hydrostatic deformation has been inferred based on tissue anatomy (Uyeno and Kier, 2005; Marshall et al., 2005), gross motor behavior (Nishikawa, 1999; McClung and Goldberg, 2000) and electromyographic recordings (Bailey and Fregosi, 2001). We propose that lingual hydrostatic deformation is best considered mechanically if the tissue is portrayed as a set of coupled units of compression and expansion. The technique of tagged magnetization MRI provides a basis to demonstrate the internal deformation patterns of the human tongue. This method applies a grid-like array of crossing bands of saturated magnetization and from the deformation of these bands during tissue motion generates spatially resolved 3-D



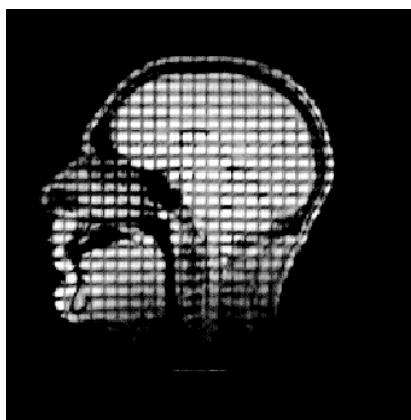


Fig. 8. Tagged magnetization to assess local tissue deformation. Saturated longitudinal magnetization is applied in two orthogonal directions, which from the sagittal planar perspective (shown here) appears as a rectilinear grid of dark bands amidst the relative brightness of the rest of the MR image. Strain is determined in image post-processing by measuring the amount of deformation undergone by these bands of magnetization during the course of tissue motion.

strain maps (Fig. 8). Since the relative brightness of a pixel (in a proton density-weighted image) is due principally to the amount of longitudinal magnetization just prior to the imaging pulse sequence, tissue affected by the tagging pulses appears dark in contrast to the surrounding tissue. Deformation is

quantified in image post-processing with non-linear Green's strain tensor. In order to resolve the idealized material continuum of the tongue, discrete triangular deforming elements are defined by digitizing nodes at tag line intersections (Fig. 9). Each triangular element is thus composed of two independently deforming line elements: one along the  $x$ -axis and the other along the  $y$ -axis in the rest configuration. The length of each line segment is defined at rest by the tag spacing. Axial strains are calculated based on the lengths of the deformed line elements, while shear strain may be calculated based on line element lengths, as well as the relative angle between adjacent line elements. Although this tagging technique is inherently 2-D, out-of-plane axial strain may be calculated by knowing the 2-D strain condition, assuming that tongue muscle is incompressible and that out-of-plane shear strains are negligible. Since shear strains are assumed to be nil, each finite triangular element in the tagging grid has an associated non-linear symmetric strain tensor. The resulting strain map constitutes a pseudosurface whose height at a given spatial location is defined by the amount of strain at that location, as determined by its proximity to a finite element centroid. The entire strain tensor may then be represented by a set of octahedra, with each octahedron centered on a tagging element's centroid and the major and minor axes oriented according to the directions of the eigenvectors and scaled to directional axial stretch.

Employing this approach, Napadow et al. (Napadow et al., 1999a) demonstrated that anterior tongue protrusion results

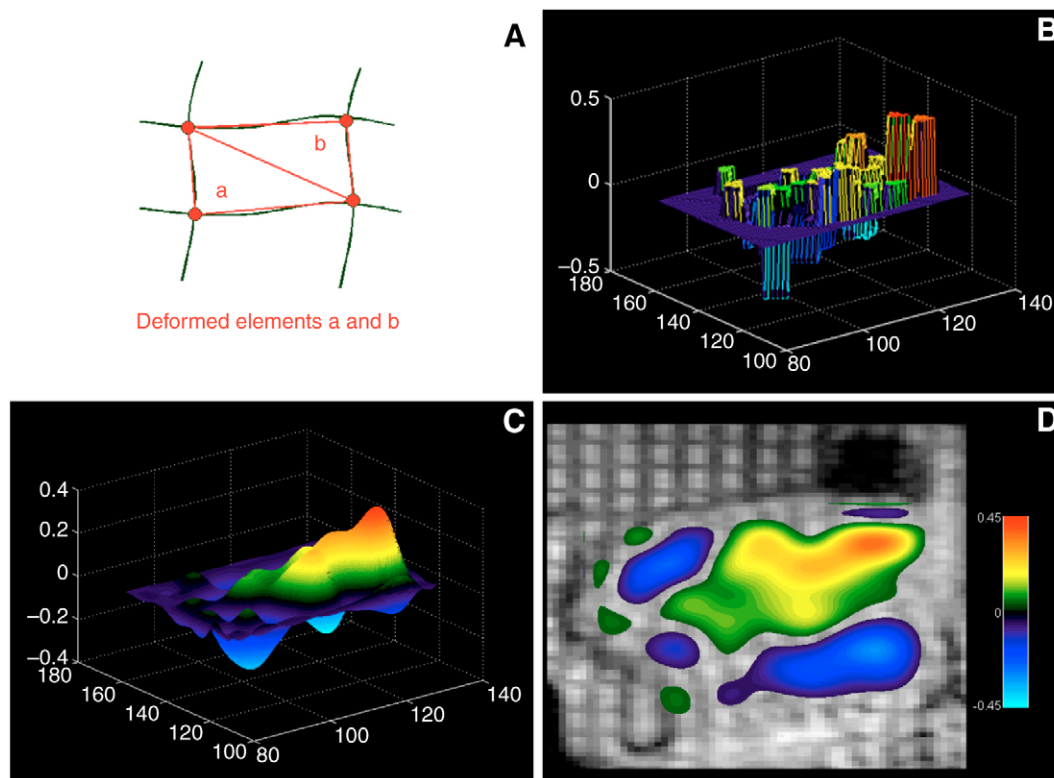


Fig. 9. Visualization of strain derived from tagged magnetization. (A) To obtain local strain from tagged magnetization images, triangular elements are defined by digitizing nodes at tag line intersections. (B) Strain is represented as a pseudosurface whose height denotes the amount of strain for each element of the mesh. (C) The surface is smoothed by the application of a bicubic spline algorithm. (D) The surface is rotated and viewed from above, where the pseudosurface becomes a color-coded strain map.

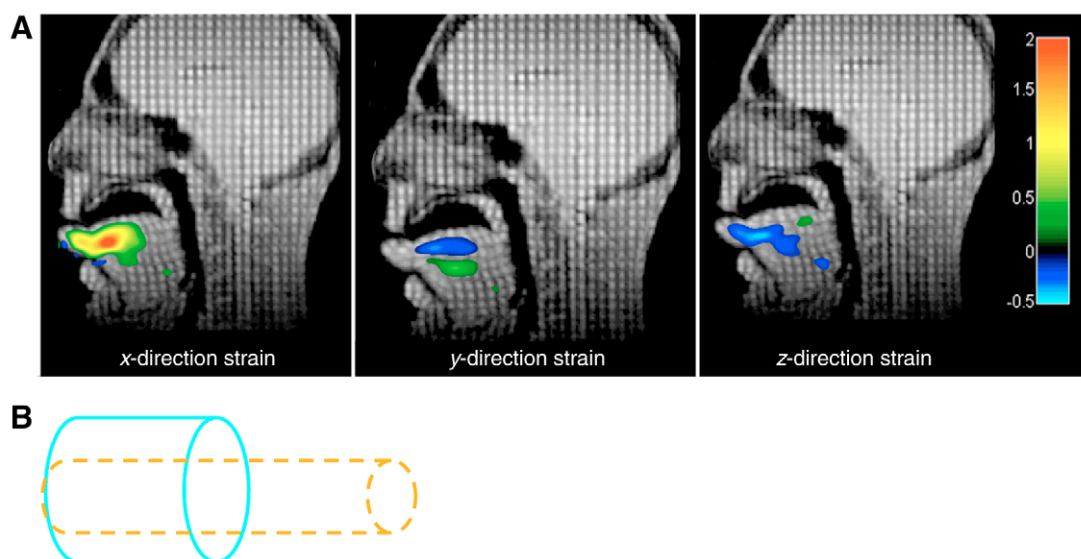


Fig. 10. Tagged magnetization depicting 3-D strain associated with anterior protrusion of the human tongue. (A) A grid of supersaturated MRI tags was applied to the resting tongue in the mid-sagittal imaging plane, and principal strain depicted for the  $x$ ,  $y$  and  $z$  components of the strain tensor in terms of a color-coded pseudosurface smoothed by bicubic splines. A bidirectional contraction in the  $y$ - and  $z$ -directions resulted in tissue protrusion in the  $x$ -direction. (B) Model of bidirectional contraction leading to hydrostatic elongation. Contraction of muscle fibers orthogonally aligned to each other results in hydrostatic elongation in the remaining direction (dashed lines), without a change in tissue volume. (Reproduced with permission from Napadow et al., 1999a.)

from simultaneous bi-directional contraction of the transversely and vertically oriented muscles of the lingual core, resulting in anterior extension due to tissue incompressibility (Fig. 10). A model may thus be generated whereby bi-directional contraction of orthogonal fibers in the intrinsic core of the tongue causes an expansion along the tongue's long axis due to the relative incompressibility of the tissue. Contraction in the tongue core occurred in the superior–inferior and medial–lateral directions, as inferred from the region's fiber orientation. For this simple prototypical motion, negative strain presented in these directions may be considered synonymous with muscle contraction because overlapping extrinsic muscle attachments lateral or superior to the regions in question were non-existent. Such attachments could conceivably introduce compressive strain to uncontracted muscle tissue by deforming adjacent muscle fibers in the organ. Bending of the tongue, either upward or laterally, is caused by regional bidirectional contraction of the core fibers as above, combined with unilateral contraction of the longitudinal sheath (Fig. 11). Contraction of the longitudinal muscle fibers on the side of the tongue closest to the center of curvature may be demonstrated by the existence of negative strain values at the inside edge. These results thus support the prediction made by Smith and Kier (Smith and Kier, 1989) that unilateral contraction of the peripherally located and longitudinally oriented sheath is a mechanism for bending in a muscular hydrostat. These data additionally demonstrate a synergistic mechanism for tissue bending through graded core fiber contraction as a function of radial distance from the center of curvature. The graded pattern of contractility may exist as a summed response of medial–lateral and superior–inferior fibers, resulting in a commensurate expansion in the antero-posterior direction that increases with distance from the center of curvature and supplementing the contraction of the longitudinal

sheath in the production of bending. Similar to tongue protrusion, the region of positive superior–inferior strain seen in the sagittal bending image results from the tongue body being stretched superiorly to the hard palate.

The same MRI methods may be used to ascertain the intramural dynamics of the lingual musculature during the phases of human swallowing, including early accommodation (bolus held in the anterior oral cavity), late accommodation (bolus transferred to the posterior oral cavity) and propulsion (bolus propelled retrograde to pharynx; Fig. 12) (Napadow et al., 1999b). Early accommodation is associated with the containment of the bolus in a grooved depression in the middle portion of the tongue's dorsal surface. This grooved depression results from a synergistic contraction of the anterior genioglossus in concert with the hyoglossus, verticalis (intrinsic) and transversus (intrinsic) muscles. Verticalis contraction results from a region of negative  $y$ -direction strain in the anterior tongue. Transversus contraction may be inferred on the basis of subtle  $z$ -direction negative strain. There is, however, strong evidence of negative  $y$ -direction strain directly below the bolus, producing a depression of the containing groove. This contraction could be the result of active genioglossus contraction or a passive effect secondary to contraction of the hyoglossus inserting into the mid-portion of the tongue body, laterally and from below. The strain map demonstrates that the contractile eigenvectors (visualized as the short axes of octahedra – the direction of greatest contractile strain when  $z$ -direction strain is positive) are oriented postero-inferiorly. Since the mid-sagittal slice is directly medial to the lateral insertions of the hyoglossus, this strain pattern is consistent with either genioglossus or hyoglossus contraction. These contractions are associated with  $x$ - and  $z$ -direction expansion, elongating the grooved depression and improving bolus containment. During late accommodation, the bolus is shifted towards the posterior

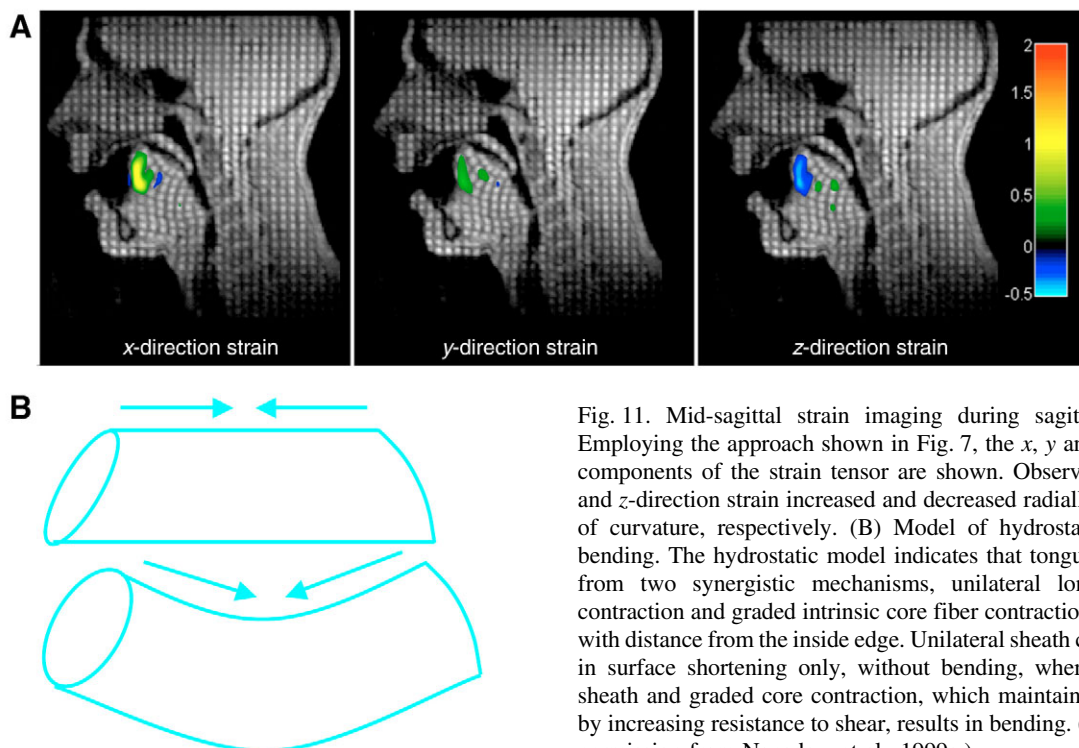


Fig. 11. Mid-sagittal strain imaging during sagittal bending. (A) Employing the approach shown in Fig. 7, the  $x$ ,  $y$  and  $z$  normal strain components of the strain tensor are shown. Observe that  $x$ -direction and  $z$ -direction strain increased and decreased radially from the center of curvature, respectively. (B) Model of hydrostatic lingual tissue bending. The hydrostatic model indicates that tongue bending results from two synergistic mechanisms, unilateral longitudinal sheath contraction and graded intrinsic core fiber contraction which increases with distance from the inside edge. Unilateral sheath contraction results in surface shortening only, without bending, whereas simultaneous sheath and graded core contraction, which maintains  $x$ -sectional area by increasing resistance to shear, results in bending. (Reproduced with permission from Napadow et al., 1999a.)

dorsal surface of the tongue, in effect ‘priming the lingual pump’ before propulsion. The most prominent finding during this phase is an increase in negative  $y$ -direction strain (i.e. inferior-directed contraction) in the posterior tongue containing the bolus. This contraction is responsible both for the creation of the posterior depression and for the extension of the bolus depression in the  $x$ - and  $z$ -directions.

Bolus propulsion reflects the net retrograde motion of the tongue, expelling the cradled bolus from the oral cavity. The most prominent effect is on the posterior tongue, with significant expansion of the tissue in the  $x$ - and  $y$ -directions and concomitant  $z$ -direction contraction. The styloglossus, which inserts into the posterior tongue body on its lateral aspects and is directed postero-superiorly towards its attachment point on the styloid process, most likely produces this universally observed strain pattern by passively dragging the tissue in the tongue’s mid-sagittal slice. This mechanism is supplemented by contraction of intrinsic transversus muscle fibers, which are also located in the posterior tongue. This contraction would cause tissue expansion in the  $x$ - and  $y$ -directions due to the incompressibility of the tongue tissue. Sole contraction of the styloglossus (in a postero-superior direction) could not produce expansive strain above its insertion point, in the mid-portion of the tongue’s lateral surfaces, since the tongue is constrained from below. Thus, styloglossus contraction would stretch the tongue tissue located between its insertion point and the tongue’s inferior attachment. Because postero-superior expansion in the posterior tongue exists all the way to the dorsal surface, a synergistic mechanism must be at work. This effect could only come from contraction of the  $z$ -directed transversus muscle in this portion of the tongue.

The demonstration of the local mechanical events associated

with human tongue deformation during protrusion, bending and the phases of swallowing supports the hydrostat hypothesis in that isovolemic deformation is fostered through synergistic contractions involving orthogonally aligned fiber populations. The presence of mechanical cooperativity involving the intrinsic and extrinsic muscle groups during biologically significant motions thus provides a mechanism for isovolemic deformation.

### Integration of lingual structure and mechanical function

If lingual deformation occurs by hydrostatic means, functional models may represent tissue deformation as a set of local isovolemic changes. Muscle incompressibility implies that shortening in one or several directions due to contraction should be compensated for by elongation in other directions. Several investigators have developed models intended to translate existing anatomical knowledge into finite element representations for which local deformations approximate actual lingual deformations occurring during normal speech and swallowing (Kakita et al., 1985; Wilhelms-Tricarico, 1995; Sanguineti et al., 1997). These efforts substantially support the role of a complex myoarchitecture in contributing to the nominal deformations of the tongue tissue, yet do not fully address the concept of how such structures contribute to hydrostatic deformation. Within the broader biological context, various approaches have been employed in considering hydrostatic motion, although these models are limited by the fact that they describe only a limited range of dynamic behavior (Skierczynski, 1996; Kristan et al., 2000; Wilson et al., 1991) or physiological motion (Van Leeuwen and Kier, 1997), do not account for external forces such as gravity or water drag (Wadepuhl and Beyn, 1989; Alscher and Beyn, 1998) and do not include a fundamental constant volume constraint (Jordan,



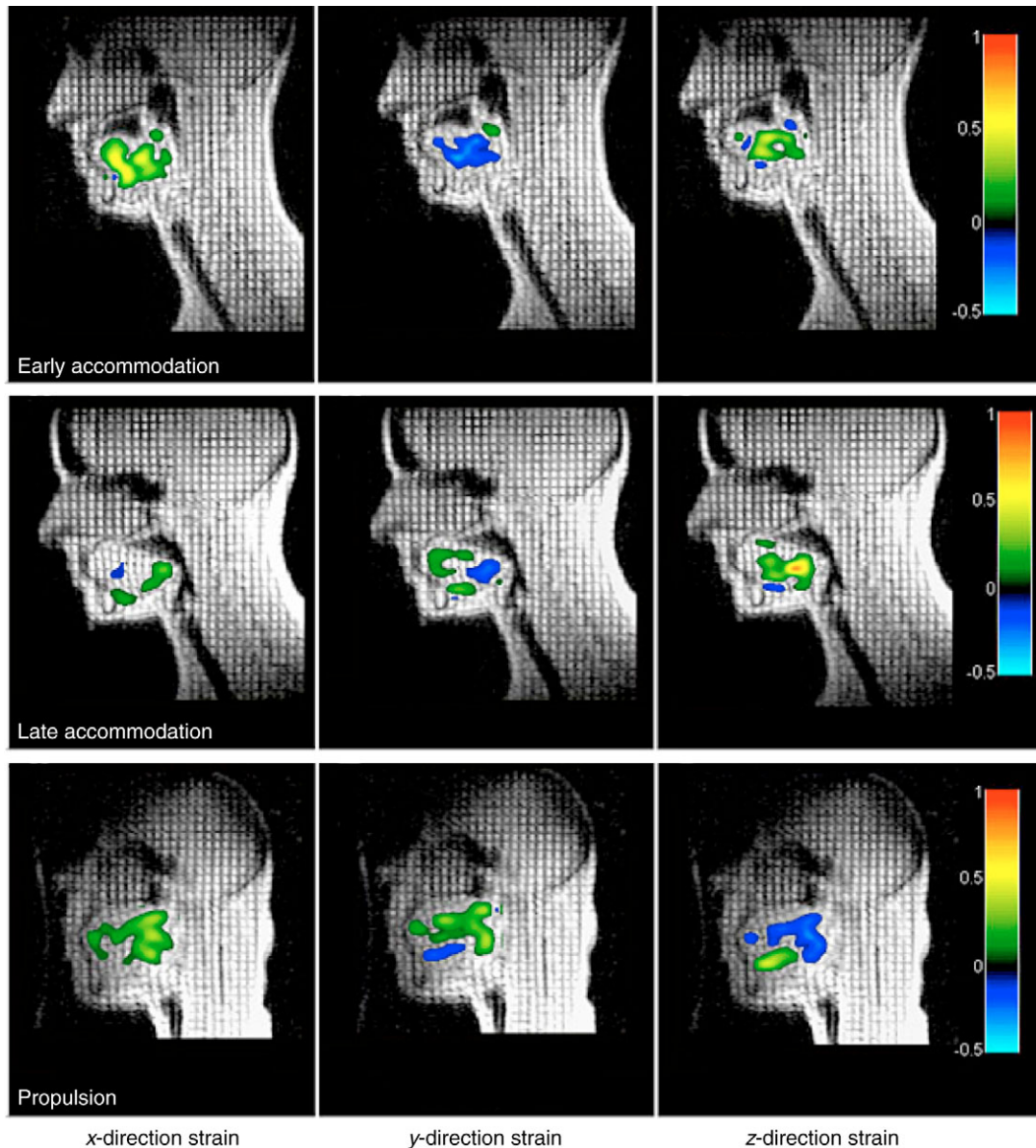


Fig. 12. Lingual strain during human swallowing. Direction-dependent strain fields were acquired for the mid-sagittal slice of the tongue during the phases of the swallow, including early accommodation (top row), late accommodation (middle row) and propulsion (bottom row). During early accommodation, bolus containment is associated with negative  $y$ -direction strain, consistent with a synergistic contraction of the anterior genioglossus and hyoglossus, with concomitant  $x$ - and  $z$ -direction expansion. During late accommodation, the combination of  $y$ -direction contraction in the posterior tongue and expansion in the anterior tongue results in shifting of the bolus to the posterior dorsal surface of the tongue, consistent principally with contraction of the posterior genioglossus and concomitant  $x$ - and  $z$ -direction expansion. During propulsion,  $x$ - and  $y$ -direction expansion in the posterior tongue was consistent with contraction of the laterally inserted styloglossus (with associated passive drag) and  $z$ -direction contraction of the posteriorly located transversus fibers. (Reproduced with permission from Napadow et al., 1999b.)

1996). On the other hand, Yekutieli and colleagues (Yekutieli et al., 2005) have described a dynamic control model of the octopus arm, similar to the tongue in that it may be modeled as a complex structure with longitudinal and transverse muscles and has the capacity for a virtually limitless array of motions. This model emphasizes the production of gross motion through internal stiffening, a phenomenon induced by the contractions of muscles orientated orthogonally to each other. However, the application of this analysis to the tongue would require an expansion of the spatial dimensions to 3-D, accounting for the application of force by the deformable tongue on the non-

deformable hard palate and the interaction of tethered (extrinsic) and untethered (intrinsic) fibers.

One of the most significant insights derived from these modeling studies is the paramount role muscular synergy plays in generating lingual deformation. For example, during anterior protrusion the transversus, verticalis and even the extrinsic genioglossus muscles play active contractile roles. In the light of our modeling results (Napadow et al., 2002), we hypothesize that the superior longitudinalis muscle also acts in concert with the above muscle groups to straighten the tongue from its resting bent configuration. Though subtle, this action is nevertheless

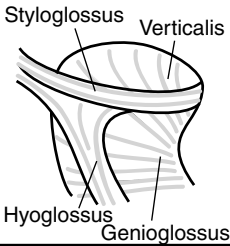

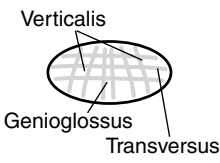

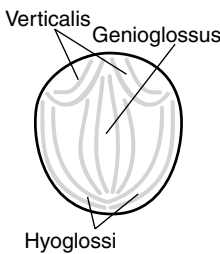

Tongue section	Rest configuration	Prototypical deformation
Sagittal		 <div>Anterior protrusion Bolus accommodation Retrograde propulsion</div>
Anterior coronal		 <div>Anterior protrusion Bolus accommodation Retrograde propulsion</div>
Posterior coronal		 <div>Anterior protrusion Bolus formation Retrograde propulsion</div>

Fig. 13. Role of muscular synergy in the generation of lingual deformation. Conceptual drawing depicting the way in which synergistic contractions involving the intrinsic and extrinsic muscles may contribute to prototypical deformations, namely anterior protrusion, bolus accommodation during swallowing and bolus propulsion during swallowing. In each instance, muscle action is viewed from the sagittal, anterior coronal and posterior coronal perspectives. In the case of anterior protrusion, a principal role is played by the simultaneous contractions of the transversus and verticalis muscles, with a secondary role played by the genioglossus (at least in the human). In the case of bolus accommodation during swallowing, a principal role is played by the midline genioglossus fibers, with a secondary role played by the longitudinalis, verticalis and transversus fibers, which serve to stiffen, broaden and bend the accommodating concavity. In the case of bolus propulsion, a synergistic role is played by the genioglossus, hyoglossus and styloglossus merging with the inferior longitudinalis, as well as the stiffening effect of bidirectional contraction of the core lingual fibers.

functionally important, and illustrates the physiological reliance of synergistic muscular synchrony in the regulation of tissue deformation. This phenomenon further supports the concept of the tongue as a muscular hydrostat. Another example of the synergistic interplay of the tongue’s muscular elements is the retrograde thrusting of the posterior tongue during the bolus propulsion stage of the swallow. This maneuver is important in clearing the bolus from the oral cavity into the oropharynx. As in other biomechanical manipulator systems in nature, synergistic muscular contractions augment physiological motion and add support and rigidity to the system. From a teleological perspective, muscular synergy may also represent a necessary adaptation for life-sustaining functions, such as feeding, control of the respiratory tract and communication. It may be shown that synergistic contractions of orthogonally aligned fibers contributes to volume-conserving tissue deformation and therefore meets one of the criteria for a muscular hydrostat. All such hydrostats possess fibers parallel and perpendicular to the organ’s long axis, but differ regarding the relative position and geometry of the perpendicular fibers. While it has been considered that the conventional concept of a hydrostat as an untethered actuator may not apply to the tongue, it may be noted that the presence of extrinsic influences does not necessarily negate the concept of hydrostatic deformation. Conceivably, extrinsically attached muscles may impose more gross deformations, as needed during propulsion, whereas the role of the intrinsic muscles may be to apply the ‘fine tuning’ needed to achieve the myriad of lingual positions, shapes and degrees of force. Synergistic contractions of extrinsic and

intrinsic muscles of the tongue, anatomically indistinct at the point of their insertion in the body of the tongue, may thus contribute to local hydrostatic effects in the human tongue.

Just how might such synergism work to create functional deformations in the tongue? While this question cannot be precisely answered with current tools, we present in Fig. 13 a series of conceptual drawings indicating which muscles might contribute to the formation of several prototypical shapes; namely, anterior-directed protrusion, bolus accommodation during swallowing and retrograde bolus propulsion during swallowing. In each case, the deformations are depicted from the sagittal, anterior coronal and posterior coronal perspectives. In each instance, the specific deformation is described from the perspective of contributions of intrinsic and extrinsic fiber populations, and is viewed in the context of its hydrostatic properties. The fact that the tissue embodies fibers with extensive and complex crossing patterns emphasizes the fact that the tissue is capable of compression or expansion in one or many directions based on the specific fiber populations that are active. Anterior protrusion appears to result principally from the synchronous contraction of the transversus and verticalis fibers. The role of the genioglossus in this rather simple deformation is controversial, but in general it appears to be less important in humans as compared to other mammalian species for which forceful extension and manipulation of the tongue is critical for obtaining food. The process of bolus accommodation is important for all mammalian species for forming the ingested morsel of food into a bolus, which then may be propelled retrograde in the course of swallowing. The exact method by

which bolus accommodation is accomplished thus defines the physical limits of oral ingestion and embodies important species-specific functionality. In this regard, note the prominent role believed to be exerted by graded contraction of the midline genioglossus fibers in humans, while also acknowledging the contribution of intrinsic fibers towards stiffening and broadening the bolus accommodating concavity. Lastly, let us consider the complex set of events contributing to the rapid and forceful reconfiguration of the tongue as it facilitates bolus movement from the oral cavity to the pharynx. Given the diverse forms and sizes taken by the bolus, it is reasonable to postulate the involvement of multiple synergisms at varying orientations to each other. It might reasonably be predicted that retrograde lingual propulsion involves the coordinated actions of the genioglossus, hyoglossus and styloglossus merging with the inferior longitudinalis, as well as the stiffening effect of bidirectional contraction of the core lingual fibers. The precise delineation of which muscles contribute to specific functional deformations of the tongue and to what degree they are active in modulating adaptive lingual mechanics will require considerable further research.

The authors gratefully acknowledge the support of National Institutes of Health grants RO1-DC05604 to R.J.G. and RO1-MH64044 to V.J.W.

## References

- Alscher, C. and Beyn, W. J. (1998). Simulating the motion of the leech: a biomechanical application of DAEs. *Numerical Algorithms* **19**, 1-12.
- Bailey, E. F. and Fregosi, R. F. (2004). Coordination of intrinsic and extrinsic tongue muscles during spontaneous breathing in the rat. *J. Appl. Physiol.* **96**, 440-449.
- Basser, P. J., Mattiello, J. and LeBihan, D. (1994). MR diffusion tensor spectroscopy and imaging. *Biophys. J.* **66**, 259-267.
- DePaul, R. and Abbs, J. H. (1996). Quantitative morphology and histochemistry of intrinsic lingual muscle fibers in *Macaca fascicularis*. *Acta Anat. Basel* **155**, 29-40.
- Flaherty, R. F., Seltzer, S., Campbell, T. A. and Weisskoff, R. M. (1995). Dynamic magnetic resonance imaging of vocal cord closure during deglutition. *Gastroenterology* **109**, 843-849.
- Gilbert, R. J., Daftary, S., Campbell, T. A. and Weisskoff, R. (1998a). Patterns of lingual tissue deformation associated with bolus containment and propulsion during deglutition as determined by echo-planar MRI. *J. Magn. Reson. Imaging* **8**, 554-560.
- Gilbert, R. J., Daftary, S., Reese, G., Weisskoff, R. M. and Wedeen, V. J. (1998b). Determination of lingual myoarchitecture in whole tissue by NMR imaging of anisotropic water diffusion. *Am. J. Physiol.* **175**, G363-G369.
- Gilbert, R. J., Magnusson, L. H., Napadow, V. J., Benner, T., Wang, R. and Wedeen, V. J. (2006). Mapping complex myoarchitecture in the bovine tongue with diffusion spectrum magnetic resonance imaging. *Biophys. J.* **91**, 1014-1022.
- Gmitro, A. F. and Alexander, A. S. (1993). Use of a projection reconstruction method to decrease motion sensitivity in diffusion weighed MRI. *Magn. Reson. Med.* **29**, 835-838.
- Hajnal, J. V., Doran, M., Hall, A. S., Collins, A. G., Oatridge, A., Pennock, J. M., Young, I. R. and Bydder, G. M. (1991). MR imaging of anisotropically restricted diffusion of water in the nervous system: technical, anatomic, and pathologic considerations. *J. Comput. Assist. Tomogr.* **15**, 1-18.
- Herrel, A., Cleuren, J. and Vree, F. (1996). Kinematics of feeding in the lizard *Agama stellio*. *J. Exp. Biol.* **199**, 1727-1742.
- Hiimae, K. M. and Palmer, J. B. (1999). Food transport and bolus formation during complete feeding sequences on foods of different consistency. *Dysphagia* **14**, 31-42.
- Jordan, C. E. (1996). Coupling internal and external mechanics to predict swimming behavior: a general approach. *Am. Zool.* **36**, 710-722.
- Kahrilas, P. J., Logemann, J. A., Lin, S. and Ergun, G. A. (1992). Pharyngeal clearance during swallowing: a combined manometric and videofluoroscopic study. *Gastroenterology* **103**, 128-136.
- Kakita, Y., Fujimura, O. and Honda, K. (1985). Computation of mapping from muscular contraction patterns in vowel space. In *Phonetic Linguistics: Essays in Honor of Peter Ladefoged* (ed. V. A. Fromkin), pp. 133-144. San Diego: Academic Press.
- Kier, W. M. and Smith, K. K. (1985). Tongues, tentacles and trunks: the biomechanics and movement of muscular hydrostats. *Zool. J. Linn. Soc.* **83**, 307-324.
- Kristan, W. B., Skalak, R., Wilson, R. J. A., Skierczynski, B. A., Murray, J. A., Eisenhart, F. J. and Cacciatore, T. W. (2000). Biomechanics of hydroskeletons: lessons learned from studies of crawling in the medicinal leech. In *Biomechanics and Neural Control of Posture and Movement* (ed. J. Winters and P. Crago), pp. 206-218. New York: Springer-Verlag.
- Lin, C. P., Wedeen, V. J., Chen, J. H., Yao, C. and Tseng, W. Y. (2003). Validation of diffusion spectrum magnetic resonance imaging with manganese-enhanced rat optic tracts and ex vivo phantoms. *Neuroimage* **19**, 482-495.
- Maddock, D. M. and Gilbert, R. J. (1993). Quantitative relationship between liquid bolus flow and laryngeal closure during deglutition. *Am. J. Physiol.* **265**, G704-G711.
- Marshall, C. D., Hsu, R. H. and Herring, S. W. (2005). Somatotopic organization of perioral musculature innervation within the pig facial motor nucleus. *Brain Behav. Evol.* **66**, 22-34.
- McClung, J. R. and Goldberg, S. J. (2000). Functional anatomy of the hypoglossal innervated muscles of the rat tongue: a model for elongation and protrusion of the mammalian tongue. *Anat. Rec.* **260**, 378-386.
- McLean, M. R. and Prothero, J. (1987). Coordinated three-dimensional reconstruction from serial sections at macroscopic and microscopic levels of resolution: the human heart. *Anat. Rec.* **219**, 374-377, 434-439.
- McLean, M. and Prothero, J. (1992). Determination of relative fiber orientation in heart muscle: methodological problems. *Anat. Rec.* **232**, 459-465.
- Miller, A. J. (1982). Deglutition. *Physiol. Rev.* **62**, 129-184.
- Moseley, M. E., Kucharczyk, J., Asgari, H. S. and Norman, D. (1991). Anisotropy in diffusion-weighted MRI. *Magn. Reson. Med.* **19**, 321-326.
- Mu, L. and Sanders, I. (1999). Neuromuscular organization of the canine tongue. *Anat. Rec.* **256**, 412-424.
- Napadow, V. J., Chen, Q., Wedeen, W. J. and Gilbert, R. J. (1999a). Intramural mechanics of the human tongue in association with physiological deformations. *J. Biomech.* **32**, 1-12.
- Napadow, V. J., Chen, Q., Wedeen, W. J. and Gilbert, R. J. (1999b). Biomechanical basis for lingual tissue deformation during swallowing. *Am. J. Physiol.* **40**, G695-G701.
- Napadow, V. J., Kamm, R. D. and Gilbert, R. J. (2002). Biomechanical model of sagittal bending for the human tongue. *J. Biomech. Eng.* **124**, 547-556.
- Nishikawa, K. C. (1999). Neuromuscular control of prey capture in frogs. *Philos. Trans. R. Soc. Lond. B Biol. Sci.* **354**, 941-954.
- Nishikawa, K. C., Kier, W. M. and Smith, K. K. (1999). Morphology and mechanics of tongue movement in the African pig-nosed *Hemisus marmoratus*: a muscular hydrostatic model. *J. Exp. Biol.* **202**, 771-780.
- Palmer, J. B., Rudin, N. J., Lara, G. and Crompton, A. W. (1992). Coordination of mastication and swallowing. *Dysphagia* **7**, 187-200.
- Paydarfar, D., Gilbert, R. J., Poppel, C. S. and Nassab, P. F. (1995). Respiratory phase resetting and airflow changes induced by swallowing in humans. *J. Physiol. Lond.* **483**, 273-288.
- Sanguineti, V., Laboisiere, R. and Payan, Y. (1997). A control model of human tongue movements in speech. *Biol. Cybern.* **77**, 11-22.
- Skierczynski, B. A., Wilson, R. J. A., Kristan, W. B. and Skalak, R. (1996). A model of the hydrostatic skeleton of the leech. *J. Theor. Biol.* **181**, 329-342.
- Smith, K. K. (1986). Morphology and function of the tongue and hyoid apparatus in Varanus (Varanidae, Lacertilia). *J. Morphol.* **187**, 261-287.
- Smith, K. K. and Kier, W. M. (1989). Trunks, tongues, and tentacles: moving with skeletons of muscle. *Am. Sci.* **77**, 29-35.
- Stejskal, E. O. (1965). Use of spin echoes in a pulsed magnetic field gradient to study anisotropic, restricted diffusion and flow. *J. Chem. Phys.* **43**, 3597-3603.
- Takemoto, H. (2001). Morphological analyses of the human tongue musculature for three-dimensional modeling. *J. Speech Lang. Hear. Res.* **44**, 95-107.
- Thexton, A. J. (1992). Mastication and swallowing. *Br. Dent. J.* **173**, 197-206.
- Thexton, A. and Hiimae, K. M. (1997). The effect of food consistency upon jaw movement in the macaque: a cineradiographic study. *J. Dent. Res.* **76**, 552-560.



- Thexton, A. J. and McGarrick, J. D.** (1988). Tongue movement of the cat during lapping. *Arch. Oral Biol.* **33**, 331-339.
- Thexton, A. J. and McGarrick, J. D.** (1994). The electromyographic activities of jaw and hyoid musculature in different ingestive behaviors in the cat. *Arch. Oral Biol.* **39**, 599-612.
- Tuch, D. S., Reese, T. G., Wiegell, M. R. and Wedeen, V. J.** (2003). Diffusion MRI of complex neural architecture. *Neuron* **40**, 885-895.
- Uyeno, T. A. and Kier, W. M.** (2005). Functional morphology of the cephalopod buccal mass: a novel joint type. *J. Morphol.* **264**, 211-222.
- Van Leeuwen, J. L. and Kier, W. M.** (1997). Functional design of tentacles in squid: linking sarcomere ultrastructure to gross morphological dynamics. *Philos. Trans. R. Soc. Lond. B Biol. Sci.* **352**, 551-571.
- Wadepuhl, M. and Beyn, W. J.** (1989). Computer simulation of the hydrostatic skeleton. The physical equivalent, mathematics and application to worm-like forms. *J. Theor. Biol.* **136**, 379-402.
- Wedeen, V. J., Reese, T. G., Tuch, D. S., Wiegell, M. R., Dou, J.-G., Weisskoff, R. M. and Chessler, D.** (2000). Mapping fiber orientation spectra in cerebral white matter with Fourier-transform diffusion MRI. In *Proceedings of the 8th Meeting of the International Society for Magnetic Resonance in Medicine, Denver, Colorado, April 3-7, 2000*. Berkley, CA: International Society for Magnetic Resonance in Medicine.
- Wedeen, V. J., Reese, T. G., Napadow, V. J. and Gilbert, R. J.** (2001). Demonstration of primary and secondary fiber architecture of the bovine tongue by diffusion tensor magnetic resonance imaging. *Biophys. J.* **80**, 1024-1028.
- Wilhelms-Tricarico, R.** (1995). Physiological modeling of speech production: methods for modeling soft tissue articulators. *J. Acoust. Soc. Am.* **97**, 3085-3098.
- Wilson, J. F., Mahajan, U., Wainwright, S. A. and Croner, L. J.** (1991). A continuum model of elephant trunks. *J. Biomech. Eng.* **113**, 79-84.
- Wu, J. C., Wong, E. C., Arrindell, E. L., Simons, K. B., Jesmanowicz, A. and Hyde, J. S.** (1993). In vivo determination of the anisotropic diffusion of water and the T1 and T2 times in the rabbit lens by high-resolution magnetic resonance imaging. *Invest. Ophthalmol. Vis. Sci.* **34**, 2151-2158.
- Yekutieli, Y., Sagiv-Zohar, R., Aharonov, R., Engel, Y., Hochner, B. and Flash, T.** (2005). Dynamic model of the octopus arm. I. Biomechanics of the octopus reaching movement. *J. Neurophysiol.* **94**, 1443-1458.